

Surface-coupling of Cerenkov radiation from a modified metallic metamaterial slab via Brillouin-band folding

Anirban Bera,¹ Ranjan Kumar Barik,¹ Matlabjon Sattorov,^{2,3} Ohjoon Kwon,^{2,3} Sun-Hong Min,^{2,3} In-Keun Baek,² Seontae Kim,² Jin-Kyu So,⁵ and Gun-Sik Park^{1,2,3,4,*}

¹School of Electrical Engineering and Computer Science, Seoul National University, Seoul 151-747, South Korea

²Center for THz-Bio Application Systems, Department of Physics and Astronomy, Seoul National University, Seoul 151-747, South Korea

³Seoul-Teracom, Inc., Seoul-151-747, South Korea

⁴Advanced Institute of Convergence Technology, Suwon-si, Suwon-443-270, South Korea

⁵Optoelectronics Research Centre and Centre for Photonic Metamaterials, University of Southampton, High field, Southampton SO17 1BJ, UK

*gunsik@snu.ac.kr

Abstract: Metallic metamaterials with positive dielectric responses are promising as an alternative to dielectrics for the generation of Cerenkov radiation [J.-K. So et al., *Appl. Phys. Lett.* **97**(15), 151107 (2010)]. We propose here by theoretical analysis a mechanism to couple out Cerenkov radiation from the slab surfaces in the transverse direction. The proposed method based on Brillouin-zone folding is to periodically modify the thickness of the metamaterial slab in the axial direction. Moreover, the intensity of the surface-coupled radiation by this mechanism shows an order-of-magnitude enhancement compared to that of ordinary Smith-Purcell radiation.

©2014 Optical Society of America

OCIS codes: (160.3918) Metamaterials; (050.6624) Subwavelength structures.

References and links

1. D. R. Smith, J. B. Pendry, and M. C. K. Wiltshire, "Metamaterials and negative refractive index," *Science* **305**(5685), 788–792 (2004).
2. V. M. Shalaev, "Optical negative-index metamaterials," *Nat. Photonics* **1**(1), 41–48 (2007).
3. C. Enkrich, M. Wegener, S. Linden, S. Burger, L. Zschiedrich, F. Schmidt, J. F. Zhou, Th. Koschny, and C. M. Soukoulis, "Magnetic Metamaterials at telecommunication and visible frequencies," *Phys. Rev. Lett.* **95**(20), 203901 (2005).
4. G. Dolling, C. Enkrich, M. Wegener, J. F. Zhou, C. M. Soukoulis, and S. Linden, "Cut-wire pairs and plate pairs as magnetic atoms for optical metamaterials," *Opt. Lett.* **30**(23), 3198–3200 (2005).
5. Y. Liu and X. Zhang, "Metamaterials: a new frontier of science and technology," *Chem. Soc. Rev.* **40**(5), 2494–2507 (2011).
6. J. Shin, J. T. Shen, P. B. Catrysse, and S. Fan, "Cut-through metal slit array as an anisotropic metamaterial film," *IEEE J. Sel. Top. Quantum Electron.* **12**(6), 1116–1122 (2006).
7. J. T. Shen, P. B. Catrysse, and S. Fan, "Mechanism for designing metallic metamaterials with a high index of refraction," *Phys. Rev. Lett.* **94**(19), 197401 (2005).
8. J. Shin, J. T. Shen, and S. Fan, "Three-dimensional metamaterials with an ultrahigh effective refractive index over a broad bandwidth," *Phys. Rev. Lett.* **102**(9), 093903 (2009).
9. J. K. So, J. H. Won, M. A. Sattorov, S. H. Bak, K. H. Jang, G.-S. Park, D. S. Kim, and F. J. Garcia-Vidal, "Cerenkov radiation in metallic metamaterials," *Appl. Phys. Lett.* **97**(15), 151107 (2010).
10. J. K. So, K. H. Jang, G.-S. Park, and F. J. Garcia-Vidal, "Bulk and surface electromagnetic response of metallic metamaterials to convection electrons," *Appl. Phys. Lett.* **99**(7), 071106 (2011).
11. G. Andonian, O. Williams, X. Wei, P. Niknejadi, E. Hemsing, J. B. Rosenzweig, P. Muggli, M. Babzien, M. Fedurin, K. Kusche, R. Malone, and V. Yakimenko, "Resonant excitation of coherent Cerenkov radiation in dielectric lined waveguides," *Appl. Phys. Lett.* **98**(20), 202901 (2011).
12. A. M. Cook, R. Tikhoplav, S. Y. Tochitsky, G. Travish, O. B. Williams, and J. B. Rosenzweig, "Observation of narrow-band terahertz coherent Cherenkov radiation from a cylindrical dielectric-lined waveguide," *Phys. Rev. Lett.* **103**(9), 095003 (2009).

13. C. W. Neff, T. Yamashita, and C. J. Summers, "Observation of Brillouin zone folding in photonic crystal slab waveguides possessing a superlattice pattern," *Appl. Phys. Lett.* **90**(2), 021102 (2007).
14. C. W. Neff and C. J. Summers, "A photonic crystal superlattice based on triangular lattice," *Opt. Express* **13**(8), 3166–3173 (2005).
15. C. S. T. Studio Suite, 2008, <http://www.cst.com>
16. S. J. Smith and E. M. Purcell, "Visible light from localized surface charges moving across a grating," *Phys. Rev.* **92**(4), 1069 (1953).
17. T. B. Boykin and G. Klimeck, "Practical application of zone-folding concepts in tight-binding calculations," *Phys. Rev. B* **71**(11), 115215 (2005).
18. S. Nakashima and H. Harima, "Raman investigation of SiC polytypes," *Phys. Status Solidi* **162**(1), 39–64 (1997).
19. C. Palmer, *Diffraction Grating Handbook*, 6th ed. (Newport Corporation, 2005), Chap. 12.
20. O. A. Tret'yakov, "Theory of Smith-Purcell effect," *Sov. Radio Phys.* **2**, 219–223 (1966).
21. H. L. Andrews, C. H. Boulware, C. A. Brau, and J. D. Jarvis, "Gain of a Smith-Purcell free-electron laser," *Phys. Rev. ST Accel. Beams* **7**(7), 070701 (2004).

1. Introduction

In recent years, there has been great interest in exploiting the sub-wavelength resonances of structured periodic materials to create artificial electromagnetic responses in every part of the electromagnetic spectrum [1–5]. Metallic metamaterials are preferred to their dielectric counterparts from the standpoint of thermal and breakdown issues. A class of metallic metamaterials consisting of a one-dimensional array of periodic cut-through subwavelength silts perforated on a metallic slab (structure-I) as shown in Fig. 1(a), is known to exhibit a positive dielectric response [6–8]; research has demonstrated their potential as a promising platform to replace ordinary dielectric materials to generate Cerenkov radiation [9,10]. In addition, such metamaterials allow the generation of Cerenkov radiation without a kinetic energy threshold [9] and without the existence of surface electromagnetic modes [10], which is not observed in ordinary dielectrics. While the Cerenkov radiation generated in ordinary dielectric slabs is usually coupled out from the edge of the structures [11,12], this type of radiation edge coupling is not applicable to structure-I due to the near-zero group velocity of radiation in the axial direction, as explained later.

Here, in order to couple out Cerenkov radiation generated in such a metamaterial slab via what is termed Brillouin-zone folding [13,14] we propose a method that would result in the surface coupling of radiation, in contrast to the ordinary edge coupling of Cerenkov radiation, from dielectric slabs [11,12]. In the proposed method, a metamaterial slab (structure-I) is modified by changing periodically the thickness of the metamaterial slab in the axial direction, thereby introducing additional periodicity in the structure and thus proposing a new structure (structure-II) as shown in Fig. 1(b). This modification causes the guided modes supported by the metamaterial slab to become folded when viewed in the structure dispersion diagram in the radiation regime, as observed in photonic crystal possessing superlattice patterns [13].

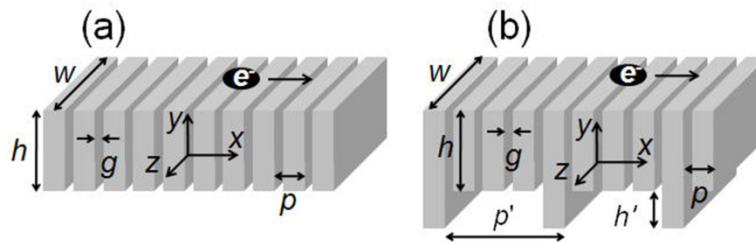


Fig. 1. (a) Metallic metamaterial structure consisting of a one-dimensional array of periodic cut-through silts perforated on a metallic slab (structure-I) in proximity to a moving electron bunch and, (b) the proposed metamaterial structure obtained by periodically modifying the thickness of structure-I so as to provide additional periodicity (structure-II).

2. Response of metallic metamaterial to convection electron

The particle-in-cell (PIC) code [15] is used to analyze structure-I in close proximity to a moving electron bunch in x direction with typical energy corresponding to a dimensionless velocity of $\beta(v/c) = 0.5$, normalized with respect to the light velocity c , and the dimensionless bunch length (σ) parameter $\sigma/p = 1/4$ of the Gaussian charge distribution. For this purpose, structure-I is modeled considering the typical dimensions of $p/g = 4$, $h/g = 10$ and $w/g = 2$, where p and g are the axial subwavelength periodicity and the width of the slits, respectively; and h and w are likewise the thickness and the width of the metal slab, with the dimensional parameter p/g corresponding to the value of the simulated refractive index of the dielectric equivalent of the metallic metamaterial, as $n (= p/g) = 4$ [7]. When this electron bunch passes near the surface of the slab (structure-I), Cerenkov radiation is generated, as can be appreciated by an anisotropic description of the metamaterial [6,9]. However, the finite thickness of the metamaterial slab enforces the generated Cerenkov radiation such that it is resonantly excited in the structure at frequencies where the guided-mode and the beam-mode phase velocities become synchronous. In order to appreciate the excitation of the guided modes and the limitation with respect to the out-coupling of generated Cerenkov radiation, we modeled and analyzed structure-I using a numerical code [15] for the guided-mode dispersion characteristics (the frequency ω versus the wave number or momentum k_x) as shown in Fig. 2(a), considering the same typical structure dimensions as already mentioned before. The approach of simulation followed here has been validated by the agreement of the results with respect to the dispersion characteristics of structure-I, agreeing within 2% with the corresponding results in the literature [6] for identical structure parameters reported therein. Further, Fig. 2(a) shows the behavior of structure-I with respect to the dispersion characteristics would correspond to the guided modes lying in the shaded region bounded by $\pm c$ -light-line, referring to the non-radiating regime. At these points of intersection between the electron beam-mode dispersion line and the guided-mode dispersion characteristics [9], plotted in Fig. 2(a), the fast Fourier transform (FFT) spectrum of structure-I, shown in Fig. 2(b), in general, exhibits the amplitude peaks of the axial component of the electric field (E_x) inside the slits (corresponding to the absence of energy radiating out of the structure); however, there were no such peaks typically beyond a limiting normalized frequency $\omega (= 2\pi c/p) = 0.32$, the absence of peaks being attributable to Smith-Purcell diffraction radiation [16] from the structure-I. In contrast, such a FFT response of structure-I far from and transverse to the structure and the electron bunch exhibits no such discernible peaks below the limiting frequency as shown in Fig. 2(b). Furthermore, the behavior of structure-I below this limiting frequency with respect to the absence of energy radiating out of the structure may also be correlated with the simulated electric field pattern at a typical frequency value that shows the confinement of the field on both the up and down surfaces of the metamaterial slab (structure-I) as shown in Fig. 2(c). In addition, there would be no power flow along the metal slab surface along x owing to the flatness of the guided-mode dispersion plot, which corresponds to the near-zero group velocity ($\partial\omega/\partial k_x \rightarrow 0$), k_x being the wave-vector (wave momentum) along x at the points of intersection between the guided-mode and the beam-mode dispersion plots as shown in Fig. 2(a).

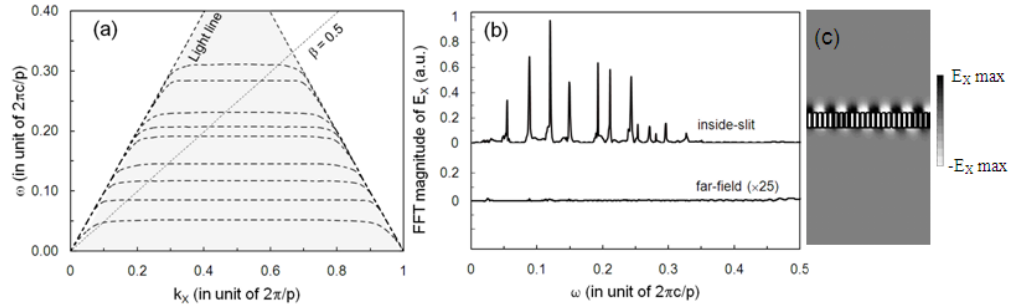


Fig. 2. (a) Guided-mode dispersion characteristics of structure-I along with a typical beam-mode dispersion line $\beta (= v/c) = 0.5$, the shaded and non-shaded regions indicating the non-radiating and radiating regimes and (b) Inside-slit and far-field (magnified 25 times) FFT spectrum of the E_x field of structure-I. (c) E_x field pattern at the typical angular frequency $\omega (= 2\pi c/p)$ of 0.12 for structure-I showing fields confined to the top and bottom surfaces.

3. Out-coupling of guided modes

The limitation of structure-I in coupling out Cerenkov radiation from the top and bottom surfaces of the structure in the transverse direction is overcome in the proposed structure-II. This is accomplished by modifying structure-I, introducing a change in the metamaterial slab thickness between h and $h + h'$ periodically at a regular interval of slits, typically four, which consequently introduces an additional periodicity ($p' = 4p$) in the axial direction of the structure geometry (structure-II) as shown in Fig. 1(b). This suggestion stems from the well known concept of the Brillouin-zone band folding phenomenon in the superlattice-based photonic crystal arising out of the reduction of the size of the first Brillouin zone of the guided-mode dispersion diagram caused by the introduction of the additional periodicity due to the larger size of the unit cell and the reduced symmetry of the crystal [13,14,17]. Let us now consider an electron bunch close to and above the top surface of structure-II moving with a velocity that is synchronous with the phase velocity of a mode supported by the structure and causing the excitation of modes in the unfolded regime of the dispersion diagram as shown in Fig. 3(a). However, it is likely that some of these modes excited in structure-II would be driven into a reduced Brillouin zone as compared to structure-I in view of the unit cell size along x of structure-II becoming p'/p times larger than that of structure-I, which is therefore likely to result in the folding of the guided modes at $k_x = \pi/p'$ [18]. Figure 3(a) shows the folded bands which are obtained by translating the guided bands of structure-I by an appropriate reciprocal lattice vector conforming to the Brillouin-zone folding effect [14,17,18]. In the present context, the wave number (momentum) of each of the modes, lying on the positive side of the band-folding symmetry ($k_x = \pi/p'$) on the momentum (k_x) scale [17,18], is translated into negative side of the band-folding symmetry, with the guided-mode frequency remaining unchanged as shown in Fig. 3(a). The amount of this translation is equal to the separation between the point of symmetry $k_x = \pi/p'$ and the momentum of the guided mode.

Typically, out of the first four guided modes of structure-II excited by the electron bunch at the angular frequencies $\omega (= 2\pi c/p)$ of 0.05, 0.085, 0.12 and 0.145, respectively, while the first of these excited modes at $\omega (= 2\pi c/p) = 0.05$ remains in the unfolded regime, the remaining three are in the folded regime with their respective momenta shifted through band folding from the unfolded regime. Further, out of the three modes in the folded regime, while one, at $\omega (= 2\pi c/p) = 0.085$, is in the guided regime ($k_x > \omega/c$), the remaining two modes, at $\omega (= 2\pi c/p) = 0.12$ and 0.145, are within the light zone ($k_x < \omega/c$), which would exhibit far-field peaks in the FFT spectrum at these two frequencies corresponding to the far-field radiation from structure-II. Figure 3(b) shows the FFT spectrum far field radiation from structure-II. The phenomenon of the coupling out of radiation can also be appreciated from

the E_x -field pattern of structure-II, typically illustrated at $\omega(=2\pi c/p)=0.12$ as shown in Fig. 3(c) vis-à-vis the corresponding field pattern of structure-I showing no such radiation as shown in Fig. 2(c).

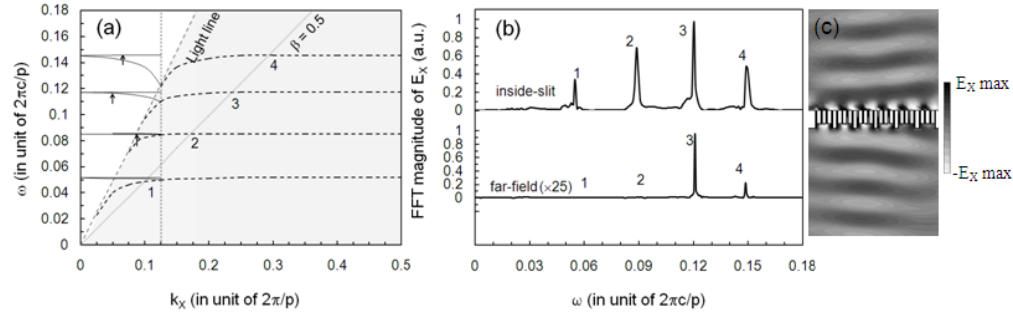


Fig. 3. (a) Guided-mode dispersion characteristics of structure-II, along with a typical beam-mode dispersion line $\beta(=v/c)=0.5$, the shaded and non-shaded regions indicating the non-radiating and radiating regimes, respectively. The first four lower dispersion intersecting points are represented by 1, 2, 3 and 4, respectively. The folded bands are shown in solid lines, with the vertical dotted line indicating band-folding symmetry and with the points indicated by the arrows on the folded dispersion curve representing the points at which the momentums corresponding to points 2, 3 and 4, respectively, are shifted due to band folding. (b) Inside-slit and far-field (magnified 25 times) FFT spectrum of the E_x field of structure-II. (c) E_x field pattern at the typical angular frequency ($\omega=2\pi c/p$) of 0.12 for structure-II showing fields radiated from the top and bottom surfaces.

4. Comparison of radiation intensity with that of reflection grating

The radiation intensity, measured in terms of the square of the amplitude of the axial electric field, from structure-II is compared to that from a reflection grating [19] under identical conditions. Figure 4 shows the comparison of radiation intensity of structure-II with that of reflection grating. For this purpose, we consider both the structures in close proximity to a moving electron bunch of typical energy corresponding to the dimensionless axial velocity $\beta(v/c)=0.5$. We also consider the identical axial periodicity (p') and identical width (w) for the reflection grating and optimize its groove depth to the value of $H'=0.44p'$, as indicated in the inset of Fig. 4, at an angular frequency $\omega(=2\pi c/p)=0.12$, for the maximum Smith-Purcell radiation intensity in a direction normal to the grating surface. At this frequency, structure-II also shows the far-field peak as shown in Fig. 3(b). It is clearly seen from Fig. 4 that the proposed structure-II is superior to the reflection grating in term of the intensity of the radiation. This enhanced radiation capability of structure-II in comparison with the reflection grating can be attributed to the phenomenon of coupling of Cerenkov radiation generated via Brillouin-zone band folding in structure-II, which is absent in the reflection grating where the surface electromagnetic waves supported by a grating are known to be excited by the moving electron bunch, and which, however, cannot contribute to the far-field radiation [20,21].

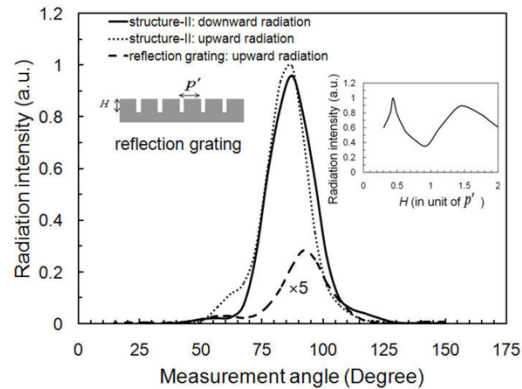


Fig. 4. Angular dependence of the far-field radiation of structure-II compared to that of the reflection grating (magnified 5 times) at an angular frequency $\omega(=2\pi c/p)$ of 0.12, the measurement angle being the angle between the direction of the moving electron bunch and that of the radiation, with the inset showing the variation of the radiation intensity of the reflection grating with the grating groove depth having a moving electron bunch energy level corresponding to $\beta(=v/c)=0.5$.

4. Conclusion

We have demonstrated that Cerenkov radiation generated inside metallic metamaterial slabs can be out-coupled via the mechanism of Brillouin-zone band folding and implemented by the proposed new structure, which is essentially a modified metamaterial slab (structure-I) in which additional periodicity is introduced (structure-II). The new structure interacting with a moving electron bunch proves to be better than the reflection grating structure with respect to the radiation intensity from the structure. The structure, being metallic, appears to enjoy an obvious edge over any dielectric Cerenkov device in terms of circumventing adverse effects such as the dielectric breakdown, the dielectric charging that incurs heating if the dielectric is lossy, and the issues arising from the cooling of the device. All-metal metamaterial structure studied in this paper can be a good candidate as an interaction structure for a terahertz source.

Acknowledgments

This work was supported in part by the Central Electronics Engineering Research Institute, Pilani, India; in part by National Research Foundation of Korea (NRF) grant funded by the Korea government (MSIP) (No. 2009-0083512) and by the World Class Institute (WCI) Program of the National Research Foundation of Korea (NRF) funded by the Ministry of Science, ICT and Future Planning. (NRF Grant Number: WCI 2011-001).